

## A short-term chick embryo *in vivo* xenograft model to study retinoblastoma cancer stem cells

Rohini M Nair<sup>1,2\*</sup>, Narayana VL Revu<sup>1\*</sup>, Sucharita Gali<sup>1</sup>, Prathap Reddy Kallamadi<sup>3</sup>, Varsha Prabhu<sup>1</sup>, Radhika Manukonda<sup>1</sup>, Harishankar Nemani<sup>3</sup>, Swathi Kaliki<sup>4,5</sup>, Geeta K Vemuganti<sup>1</sup>

**Purpose:** Cancer stem cells (CSCs) reported in various tumors play a crucial role in tumorigenesis and metastasis of retinoblastoma (Rb). Following the efforts to reduce, replace, and refine the use of mammalian models, we aimed to establish a short-term xenograft for Rb to evaluate the CSC properties of CD133<sup>+</sup> Rb Y79 cells, using the well-established chick embryo chorioallantoic membrane (CE-CAM) assay. **Methods:** Y79 cells were cultured, labeled with two different dyes (CM-Dil Y79 and enhanced green fluorescent protein (eGFP)) and sorted for CD133<sup>+</sup> and CD133<sup>-</sup> subsets. Two million cells from each of the labeled groups were transplanted onto the abraded CAM on embryonic day 7 (E7). On E14, the tumor nodule formation on CAM and spontaneous metastasis to the embryos were evaluated by confocal microscopy, *in vivo* imaging, and histology. **Results:** Y79 cells formed pink-white raised perivascular nodules with feeder vessels on the CAM with both the types of labeled CD133<sup>+</sup> cells. CD133<sup>-</sup> cells, when compared to CD133<sup>+</sup> cells, demonstrated significantly larger tumor volume ( $40.45 \pm 7.744 \text{ mm}^3$  vs  $3.478 \pm 0.69 \text{ mm}^3$ ,  $P = 0.0014$ ) and higher fluorescence intensity (CM-Dil: AUF =  $6.37 \times 10^7 \pm 7.7 \times 10^6$  vs  $1.08 \times 10^7 \pm 1.6 \times 10^6$ ;  $P < 0.0001$ ; eGFP: AUF =  $13.94 \times 10^4 \pm 2.54 \times 10^4$  vs AUF =  $1.39 \times 10^4 \pm 0.4 \times 10^4$ ;  $P = 0.0003$ ). The metastatic potential of CD133<sup>-</sup> cells was also observed to be higher as noted by *in vivo* imaging and histopathology. **Conclusion:** This study highlights that CE-CAM is a feasible alternative nonmammalian model for evaluating tumorigenicity and metastatic potential of Y79 CSCs. Increased tumorigenicity and metastatic potential of CD133<sup>-</sup> subset of tumor cells substantiate their CSC properties.

**Key words:** Cancer stem cells, chick embryo, metastasis, retinoblastoma, Xenograft model

Retinoblastoma (Rb) is the most common intraocular pediatric tumor that affects the developing retina, caused predominantly due to mutations in the *RB1* gene.<sup>[1]</sup> Survival with the precise and timely diagnosis with treatment is as high as 95%, but when left untreated, the disease can be fatal.<sup>[2]</sup> Rb can occur in one or both the eyes, and advanced bilateral Rb is very difficult to treat owing to tumor cell invasion into the vitreous, subretinal space and aqueous chamber with high chances of extraocular metastasis.<sup>[3,4]</sup> Therefore, it is imperative to understand the tumorigenesis and invasive nature of Rb cells to design effective treatment strategies. Cancer stem cells (CSCs), a subset of cancer cells, have been identified as an important driver of tumorigenesis, metastasis, and even therapeutic resistance in several cancers.<sup>[5,6]</sup> In our attempt to investigate the role of CSCs in Y79 cell line, we had demonstrated that FSC<sup>lo</sup>/SSC<sup>lo</sup>/CD133<sup>lo</sup> subset has the properties of CSCs *in vitro* such

as colony-forming ability, differentiation, chemoresistance, invasion, and stem cell-specific gene expression signature.<sup>[7,8]</sup> Translation of *in vitro* studies to *in vivo* model systems has become an integral part of functional tumor biology studies and clinically relevant model systems help in developing better treatment strategies.<sup>[9]</sup> Several genetic and xenograft animal models have been established to explore Rb tumorigenesis, metastasis, and targeted therapies.<sup>[10]</sup> The genetic models have been developed based on knockout strategies of key *Rb*-related genes such as *p107*, *p130*, *p53*, and overexpression of oncogenes such as *Chx 10* and *Pax 6*.<sup>[11]</sup> Several orthotopic and xenograft rodent models have also been developed; however, the major disadvantage of these models is the lag time of tumor development and resemblance to native human Rb tumorigenesis. The chick embryo-chorioallantoic membrane (CE-CAM) model has been the model of choice for tumor xenograft studies for over a century, owing to its naturally immunodeficient state, ease of manipulation, visualization, and short growth period.<sup>[12,13]</sup> The CE-CAM model has been explored for ocular tumors; however, its

<sup>1</sup>School of Medical Sciences, University of Hyderabad, Hyderabad, India, <sup>2</sup>Department of Ophthalmology, Perelman School of Medicine, University of Pennsylvania, Philadelphia, United States, PA, <sup>3</sup>Animal Facility, National Institute of Nutrition, Hyderabad, <sup>4</sup>The Operation Eyesight Universal Institute for Eye Cancer, L V Prasad Eye Institute, Hyderabad, <sup>5</sup>Ophthalmic Pathology Laboratory, L V Prasad Eye Institute, Hyderabad, India

\*Both Rohini M Nair and Narayana VL Revu contributed equally as first authors

**Correspondence to:** Prof. Geeta K. Vemuganti, University of Hyderabad, Prof CR Road, Gachibowli, Hyderabad, Telangana, India. E-mail: gkvemuganti@gmail.com

Received: 08-Sep-2021

Revision: 17-Oct-2021

Accepted: 14-Jan-2022

Published: 28-Apr-2022

Videos Available on:  
www.ijo.in

Access this article online

Website:  
www.ijo.in

DOI:  
10.4103/ijo.IJO\_2348\_21

Quick Response Code:



This is an open access journal, and articles are distributed under the terms of the Creative Commons Attribution-NonCommercial-ShareAlike 4.0 License, which allows others to remix, tweak, and build upon the work non-commercially, as long as appropriate credit is given and the new creations are licensed under the identical terms.

**For reprints contact:** WKHLRPMedknow\_reprints@wolterskluwer.com

**Cite this article as:** Nair RM, Revu NV, Gali S, Kallamadi PR, Prabhu V, Manukonda R, et al. A short-term chick embryo *in vivo* xenograft model to study retinoblastoma cancer stem cells. Indian J Ophthalmol 2022;70:1703-11.

potential to validate the Rb CSC properties has not been evaluated.<sup>[14–16]</sup>

In this study, we aimed to establish a CE-CAM xenograft model system for investigating the role of Rb CSCs from Y79 cell line in promoting tumorigenesis and spontaneous metastasis assessed by gross, confocal, *in vivo* imaging and histological techniques.

## Methods

### Cell culture

Y79 cell line (Riken: RCB1645) and enhanced green fluorescent protein (eGFP) Y79 were generous gifts from Dr. S. Krishnakumar (Sankara Nethralaya, India) and Prof Sarah E Coupland (Liverpool Ocular Oncology Research Group, University of Liverpool, UK), respectively. The cells were grown in complete growth media composed of RPMI-1640 (Gibco™, Thermo Fisher Scientific, USA) medium supplemented with 10% fetal bovine serum (FBS) (Gibco™, Thermo Fisher Scientific, USA) and 1X antibiotic–antimycotic solution (Gibco™, Thermo Fisher Scientific, USA). The cells were cultured at 5% CO<sub>2</sub> and 37°C until they reached over 80% confluence following which they were used for the experiments.

### Magnetic activated cell sorting (MACS) and flow cytometry

Cultured Y79 cells and eGFP Y79 cells were sorted using CD133 micro bead kit according to manufacturer's protocol (MiltenyiBiotec Inc., Auburn, CA) as described previously.<sup>[7]</sup> Briefly, the cells were washed with MACS buffer (2 mM EDTA and 0.5% FBS containing phosphate- buffered saline (PBS); pH – 7.2), and resuspended in 300 µL of MACS buffer. One hundred microliters of FcR blocking reagent and 100 µL of CD133 micro beads were added and incubated for 30 min at 4°C for CD133 magnetic labeling. The cell mixture was passed through the LS mini MACS columns followed by the repeated washes with MACS buffer; CD133<sup>-</sup> cells were eluted first and collected in tube with media. The columns were removed from the MACS magnet, and CD133<sup>+</sup> cell fractions were eluted out using MACS buffer. Both the cell populations were concentrated and resuspended in 1 mL of serum free media. The cell count and cell viability of post MACS were assessed by a Neubauer chamber. The purity of the sorted cells was analyzed by flow cytometry (BD LSRFortessa™).

### Labeling of Y79 cells

For xenograft studies, two approaches of fluorescent cell tracking were utilized and their staining intensities were analyzed *in vitro* prior to transplantation. The sorted Y79 cells were labeled using lipophilic carbocyanine red dye CM-Dil (ThermoFisher Scientific, USA). Briefly, the cells were washed and resuspended in 1 mL serum free media. The cells were stained with 5 µL of CM-Dil (ThermoFisher Scientific, USA) and incubated for 20 min at 37°C. Post labeling, the cells were repeatedly washed with serum free media to remove any unconjugated dye. The labeled cells were then incubated for 2 h and assessed for staining efficiency using a fluorescence microscope prior to transplantation. The cells were also evaluated for dye retention *in vitro* for over 2 weeks.

### Chick embryo CAM assay

Embryonated white leghorn Gramapriya eggs (*G. gallus*) were procured from ICAR-Directorate of Poultry Research,

Hyderabad, India. Ethics approval was obtained by the Institutional Ethics Committee at the University of Hyderabad, and all the experiments were conducted in compliance with the ARVO Statement for the Use of Animals in Ophthalmic and Vision Research. The eggs were sterilized with 70% alcohol and incubated at 38°C and 68% relative humidity in an egg incubator (Sun Engineering, India). Growth, viability, and vascularization of eggs were monitored by candling every alternate day. On E7, a small circular window was made into the air sac of the egg using sterile microscissors. The CAM was identified by lifting the inner shell membrane and a small capillary was gently abraded. Two million cells of CM-Dil Y79 CD133<sup>-</sup> (*n* = 41), CD133<sup>+</sup> (*n* = 53) and eGFP Y79 CD133<sup>-</sup> (*n* = 10), CD133<sup>+</sup> (*n* = 10) cells in media containing Matrigel (BD Biosciences™) were transplanted on the CAM. The window was sealed back with a sterile tape and was placed in the incubator undisturbed for 7 days until dissection.

### Dissection and tumor volume of xenografts

The tumor volume measurements were performed for eGFP Y79 tumor nodules. Briefly, the window was reopened to identify tumor nodules on E14, after which the CAM and the embryo were dissected. The CAM was subjected to the evaluation of the tumor nodule, while the embryo was subjected to *in vivo* imaging. The volume of the tumor nodules on CAM (in the eGFP Y79 cells) was measured using a Vernier caliper, and volume was estimated by the following formula.<sup>[17]</sup>

$$\text{Tumor volume} = 4/3 \times \pi \times r^3 \quad (r = 1/2 \sqrt{\text{diameter}_1 \times \text{diameter}_2})$$

### CAM whole mount and confocal imaging

The CAM tissues with the tumor nodules were gently rinsed with cold PBS, placed on a glass slide and mounted with 50% glycerol for confocal analysis. The nodules were scanned on a laser scanning confocal microscope (Carl Zeiss NLO-710) at an excitation 550 nm/emission 570 nm spectrum for CM-Dil labeled cells and 488 nm/509 nm for eGFP cells. The 3D images were taken at different magnifications, and the CAM was also scanned at different range of depths using the Z-stack method. Localized depths having strong fluorescent signals were selected for image analysis by ImageJ software, and parameters were adjusted using the Zen 2010 software.

### *In vivo* imaging of whole embryos

The whole embryos were analyzed using the IVIS Spectrum *in vivo* optical imaging system (PerkinElmer) to track the presence of labeled tumor cells. The embryos transplanted with CM-Dil Y79 cells and eGFP Y79 cells were exposed to an excitation/emission spectrum of 550 nm/570 nm and 488 nm/509 nm for 30 s, respectively. Embryos transplanted with PBS solution were used as negative controls. Image display analysis was performed using Living Image software (version 4.3.1, Xenogen, Alameda, USA). Data was obtained from the fluorescent images by selecting the region of interest (ROI), and the number of photons emitted was measured as average radiance (photons/s/cm<sup>2</sup>/sr).

### Histology

The nodules with the surrounding CAM tissues were rinsed with PBS and fixed in 10% buffered formalin for 24 h. The embryos were lifted from the egg and cleaned with PBS to remove the yolk and extra embryonic membranes. The embryos were decapitated and the embryonic organs (brain,

eye, femur-bone marrow, and liver) were dissected and fixed in formalin for 24 h. Following fixation, they were processed for routine histological analysis. Immunohistochemistry was performed with Ki-67 antibody (Roche Life Sciences) to detect the proliferating Y79 tumor cells using an automated benchmark ultra IHC diagnostic system (Roche Life Sciences). Briefly, the CAM and tissue sections were deparaffinized and dipped in graded xylene solutions. Rehydration of the sections was done using graded alcohols followed by 1X PBS. A solution of methanol and hydrogen peroxidase was used to block endogenous peroxidase activity. Heat-induced antigen retrieval was done for the sections in sodium citrate buffer (pH 6). The sections were then washed with PBS and then blocked using 2.5% BSA solution. The appropriate concentration of the primary antibodies was added to the sections and incubated in a moist chamber at room temperature for 2 h. Polymer horseradish peroxidase was used as a secondary antibody, and the sections were incubated at room temperature for half an hour. The slides were then mounted with a coverslip using DPX mounting medium. The slides were then analyzed under a light microscope, and the staining was independently assessed by an experienced ocular pathologist (GKV).

### Statistical analysis

The quantitative data were stated as mean  $\pm$  SEM, and GraphPad Prism (GraphPad Software, La Jolla, CA) was used for unpaired Student's *t*-test. The representative images were analyzed using ImageJ software. The experiments were repeated at least thrice with biological replicates and  $P < 0.05$  was considered as a statistically significant difference between the groups.

## Results

### Analysis of CSCs in Y79 cells

CD133<sup>-</sup> constituted 15.5  $\pm$  0.32% of Y79 cells [Fig. 1] and CD133 expression of subsequent passages are shown in Table 1. After sorting by MACS, the CD133<sup>-</sup> and CD133<sup>+</sup> population showed a purity of  $\geq 90\%$  with 85% viability.

### *In vitro* CM-Dil fluorescent labeling and GFP transduction efficiency

The staining intensity of Y79 cells, labeled with fluorescent cell tracker CM-Dil dye was retained until 17 days in culture [Fig. 2a–c]. However, uniformity of staining within individual cells were noted to reduce as the number of days *in vitro* increased.

The eGFP-labeled Y79 cells retained GFP expression up to 2 weeks in culture. The intensity of GFP fluorescence varied cell to cell, and the majority of cells expressed GFP *in vitro* [Fig. 2d–f].

### Embryo viability and assessment of tumor formation

The survival percentages of CM-Dil Y79 transplanted embryos was 69.14% ( $n = 28$ ) and 79.71% ( $n = 41$ ), and eGFP Y79 cells

transplanted embryo viability was 90% ( $n = 9$ ) and 90% ( $n = 9$ ) for Y79 CD133<sup>-</sup> and CD133<sup>+</sup> cells, respectively. Both CM-Dil Y79 CD133<sup>-</sup> cells and eGFP Y79 CD133<sup>-</sup> cells formed pinkish-white raised wet perivascular nodules with feeder vessels on the CAM [Fig. 3a and c], whereas CD133<sup>+</sup> formed smaller plaque-like growths on the CAM [Fig. 3b and d], as observed upon gross dissection.

The tumor volume of eGFP Y79 CD133<sup>-</sup> nodules were significantly higher (40.45  $\pm$  7.744 mm<sup>3</sup>) when compared to CD133<sup>+</sup> (3.478  $\pm$  0.69 mm<sup>3</sup>,  $P = 0.0014$ ) nodules [Fig. 3e].

### Confocal imaging of tumor nodules on the CAM layer

Confocal imaging confirmed the presence of growing tumor nodules within the CAM [Fig. 4]. The fluorescence intensity from the ROI analysis showed that CAM tissue transplanted with CD133<sup>-</sup> CM-Dil Y79 cells (AUF = 6.37  $\times 10^7 \pm 2.084 \times 10^6$ ) [Supplementary Video 1] had increased localization of cells when compared to CD133<sup>+</sup> cells (AUF = 1.08  $\times 10^7 \pm 1.6 \times 10^6$ ,  $P < 0.0001$ ) [Supplementary Video 2] [Fig. 4a–c]. Similarly, the CAM tissues transplanted with CD133<sup>-</sup> eGFP Y79 cells (AUF = 4.29  $\times 10^7 \pm 1.9 \times 10^6$ ) [Supplementary Video 3] had increased localization of cells when compared to CD133<sup>+</sup> cells (AUF = 1.83  $\times 10^7 \pm 4.37 \times 10^6$ ,  $P = 0.0003$ ) [Supplementary Video 4] [Fig. 4d–f].

### *In vivo* imaging analysis of spontaneous metastasis to the embryo

The IVIS-spectral images of the chick embryos transplanted with Rb Y79 tumor cells revealed fluorescence signals in the cephalic, abdominal areas and within the bones of hind limbs. Epifluorescence signals in embryos with CD133<sup>-</sup> cells were intense and high in the abdominal region followed by the cephalic region and limbs when compared to embryos transplanted with CD133<sup>+</sup> cells [Fig. 5a, b, d, and e]. The embryos transplanted with CD133<sup>-</sup> cells showed intense and higher fluorescence with widely spread signal compared to CD133<sup>+</sup> cells for both CM-Dil and eGFP-labeled Y79 cells ( $P < 0.05$ ) [Fig. 5c and f].

### Histological analysis of the xenograft formation and metastasis

Histological examination of tumor nodules from CAM with Y79 CD133<sup>-</sup> cells revealed tumor cells which were large with high nuclear-cytoplasmic ratio, mitotic figures [Fig. 6a] with high immunoreactivity to Ki-67 [Fig. 6b]. An area of inflammatory granulation tissue was also noted. The CAM with Y79 CD133<sup>+</sup> cells showed edema, inflammatory granulation tissue, necrosis with surface ulceration [Fig. 6c], and was negative for Ki-67 [Fig. 6d]. The embryonic tissues of liver, brain, and eyes showed metastatic tumor deposits which were also immunoreactive for Ki-67 [Fig. 7a–f].

## Discussion

Rb, a childhood ocular cancer, accounts for 3% of all childhood tumors and can be fatal if left untreated owing to the rapidly growing tumor cells within the developing mutated retina.<sup>[18]</sup> Emerging evidence demonstrates the role of cancer stem cells in progression and metastasis.<sup>[19]</sup> In our earlier studies, we had demonstrated the presence of CSCs properties in the CD133<sup>-</sup> subset of cells in both primary tumors and Y79 cell line.<sup>[7,8,20]</sup> In this study, we established a short-term *in vivo* CE-CAM

**Table 1: CD133 expression of Rb Y79 cells in different passages**

Passage	% of CD133 expression
Passage-8	81.28 $\pm$ 0.86
Passage-12	83.73 $\pm$ 1.26
Passage-15	84.84 $\pm$ 1.28

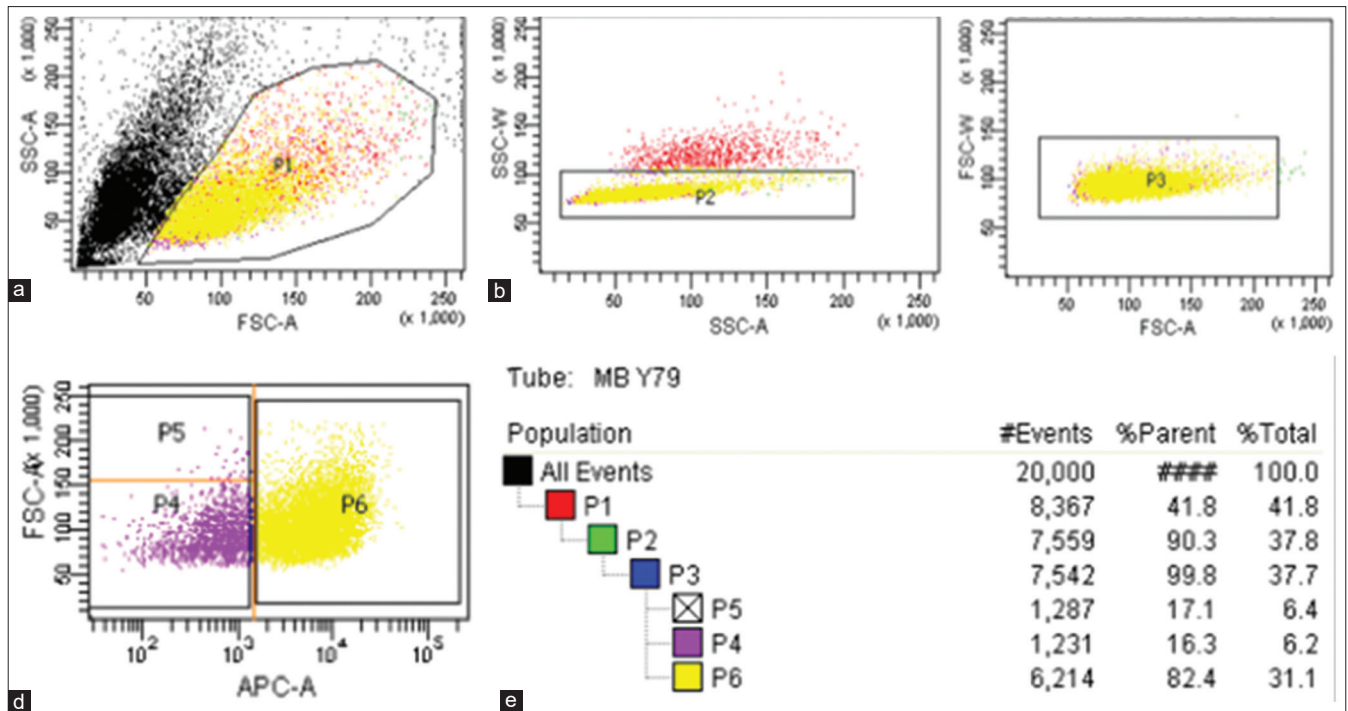


**Figure 1:** Flow cytometry analysis of CD133 expression in Rb Y79 cell line. (a) Scatter plot of Y79 cells with gating around the live population. (b and c) Doublet discrimination plots. (d) CD133-APC expression. (e) Analysis of the subpopulations

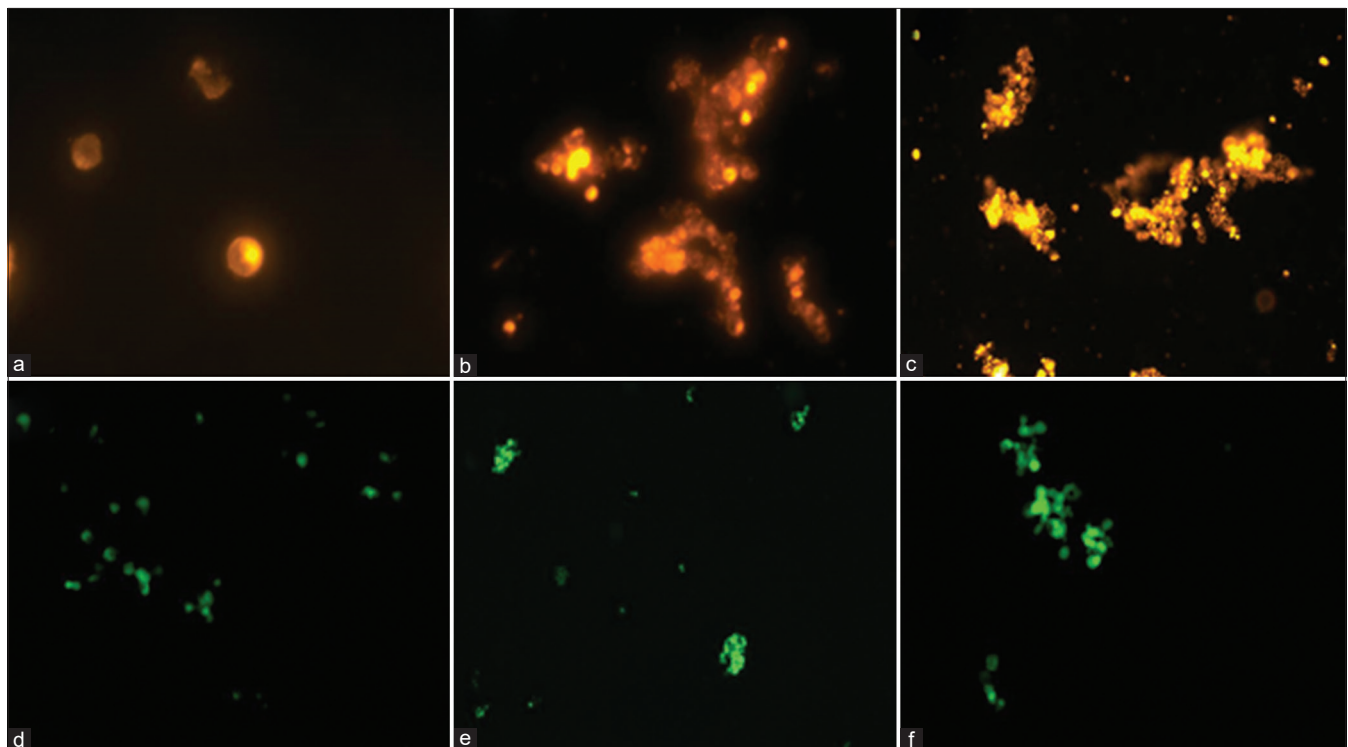


**Figure 2:** Labeling and tracking of CM-Dil Y79 cells and eGFP Y79 cells *in vitro*. CM-Dil-labeled Y79 cells in culture on day (a) 1 (40X), (b) 5, and (c) 17 days (10X) under a TRITC filter. eGFP Y79 cells in culture on day (d) 1, (e) 10, and (f) 15 days under an FITC filter (10x)

xenograft model for studying the tumorigenic and metastatic potential of labeled Y79 cells with specific reference to the CD133<sup>+</sup> subset of tumor population. The study demonstrated the successful xenograft formation on the CAM within 1 week

of transplantation with evidence of spontaneous metastasis. This xenograft model further substantiates that the CD133<sup>+</sup> subset of cells in Y79 cells are endowed with higher potential to form tumor nodules and metastases, thus conferring with CSCs properties.

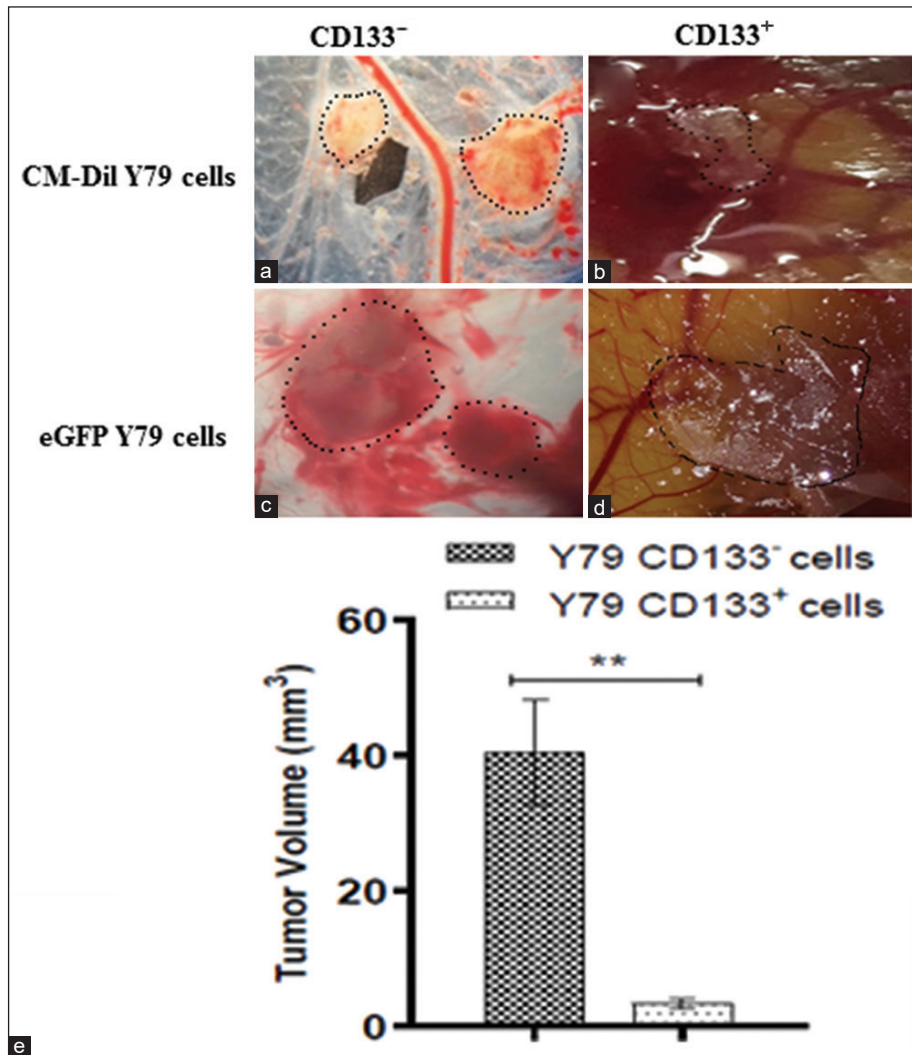


**Figure 3:** Assessment of tumor nodules formation on CAM and quantitative measurement of tumor nodules. Tumor nodules of (a) CM-Dil CD133<sup>-</sup> transplanted cells, (b) CM-Dil CD133<sup>+</sup> transplanted cells, (c) eGFP Y79 CD133<sup>-</sup> transplanted cells, and (d) eGFP Y79 CD133<sup>+</sup> transplanted cells. (e) Quantitative measurement of tumor volume of eGFP Y79 transplanted cells (CD133<sup>-</sup> vs CD133<sup>+</sup>, \*\* $P = 0.0014$ )

Animal models using transgenic and xenograft approaches have been well established for Rb.<sup>[10,18]</sup> Most of them include the mammalian system to resemble the tumor microenvironment. However, a developmental model is difficult to recapitulate in this system due to many technical difficulties.<sup>[10]</sup> The CE-CAM, therefore, offers not only a temporal investigation but also provides a reliable tool for screening therapeutics in a short duration.

Our study demonstrated the formation of tumor nodules on CAM and spontaneous metastatic spread to the embryo using CM-Dil labeled and eGFP cells. The potential of CE-CAM model in Rb studies has been explored by Busch *et al.*, who demonstrated the tumor-forming ability of various kinds of cell lines (normal and chemoresistant) in soft agar as well as CAM and also evaluated the tumor suppressor effect of the Trefoil factor family peptides in Rb cells using the CE CAM model.<sup>[14,15,21]</sup> Though the purpose of their study was toward cell line characterization and chemoresistance, the data does not provide any evidence for metastasis within the embryo. One of the possible reasons could be that the authors checked for invasion on E17/18, by which time the immune system of the embryo is

observed to be fully functional and reactive.<sup>[12]</sup> We concur with their observation of Y79 cells being capable of forming nodules on CAM and having the potential of spontaneous invasion within the CAM tissue. This observation is also similar to studies done on other solid tumors, such as glioblastoma, ovarian cancer, prostate cancer, and uveal melanoma.<sup>[16,22]</sup>

The tumor nodules formed by the Rb CSCs had the presence of feeder vessels developing around them which is a possible indication of tumor neovascularization. Ribatti *et al.*,<sup>[23]</sup> demonstrated the presence of multiple host vessels around and within the tumor nodule in a neuroblastoma CAM xenograft model, suggesting that tumor cells were capable of inducing angiogenesis using the chorioallantoic vasculature. This could also serve as an important model to enhance or suppress Rb angiogenesis in tumor models due to its ease of visualization.

The presence of spontaneous tumor metastasis was observed in the cephalic, abdominal, and limb regions of the embryo using the whole embryo *in vivo* imaging and confirmed by histology in the sections of embryonic organs such as the brain,

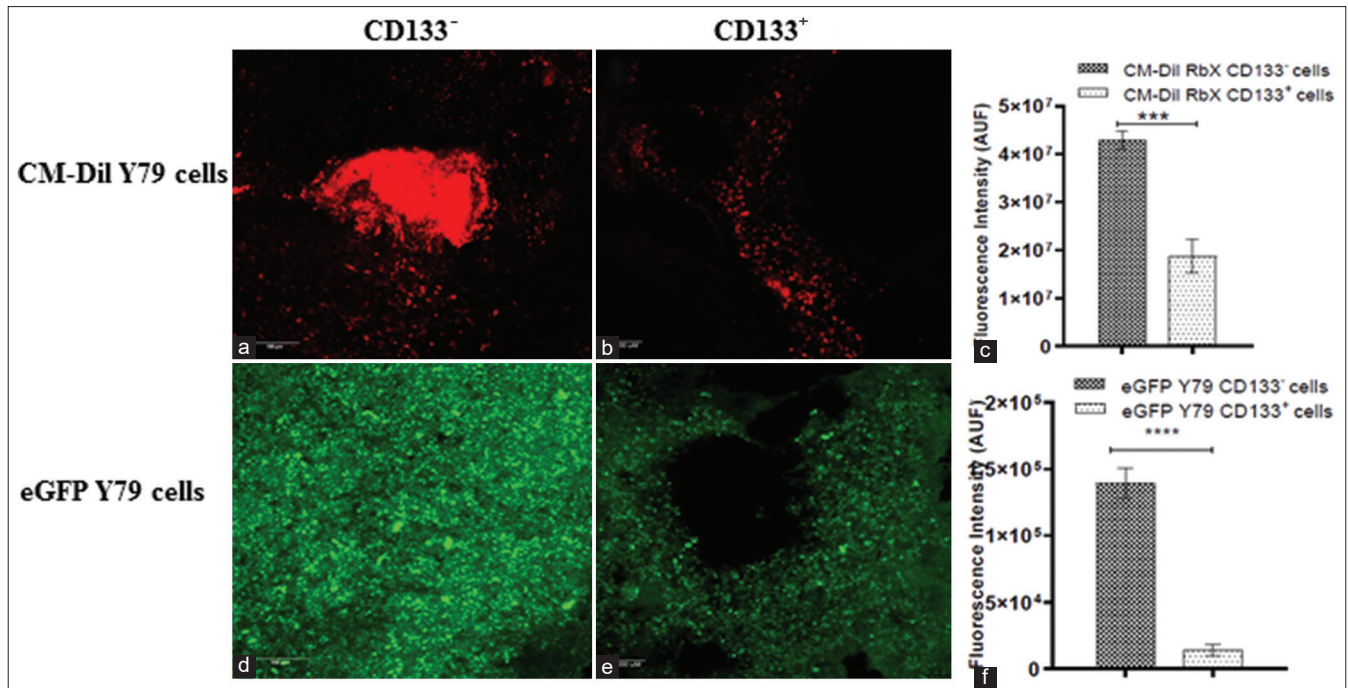


**Figure 4:** Confocal imaging and analysis of tumors formed on the CAM layer. Representative confocal images of CAM nodules formed by (a) CM-Dil Y79 CD133<sup>-</sup> cells, (b) CM-Dil Y79 CD133<sup>+</sup> cells, (d) eGFP Y79 CD133<sup>-</sup> cells, (e) eGFP Y79 CD133<sup>+</sup> cells. Quantification of fluorescence showed that the CD133<sup>-</sup> cells of CM-Dil Y79 (c) and eGFP Y79 (f) displayed an increased localization compared to their CD133<sup>+</sup> counterparts (\*\*\*\**P* < 0.0001)

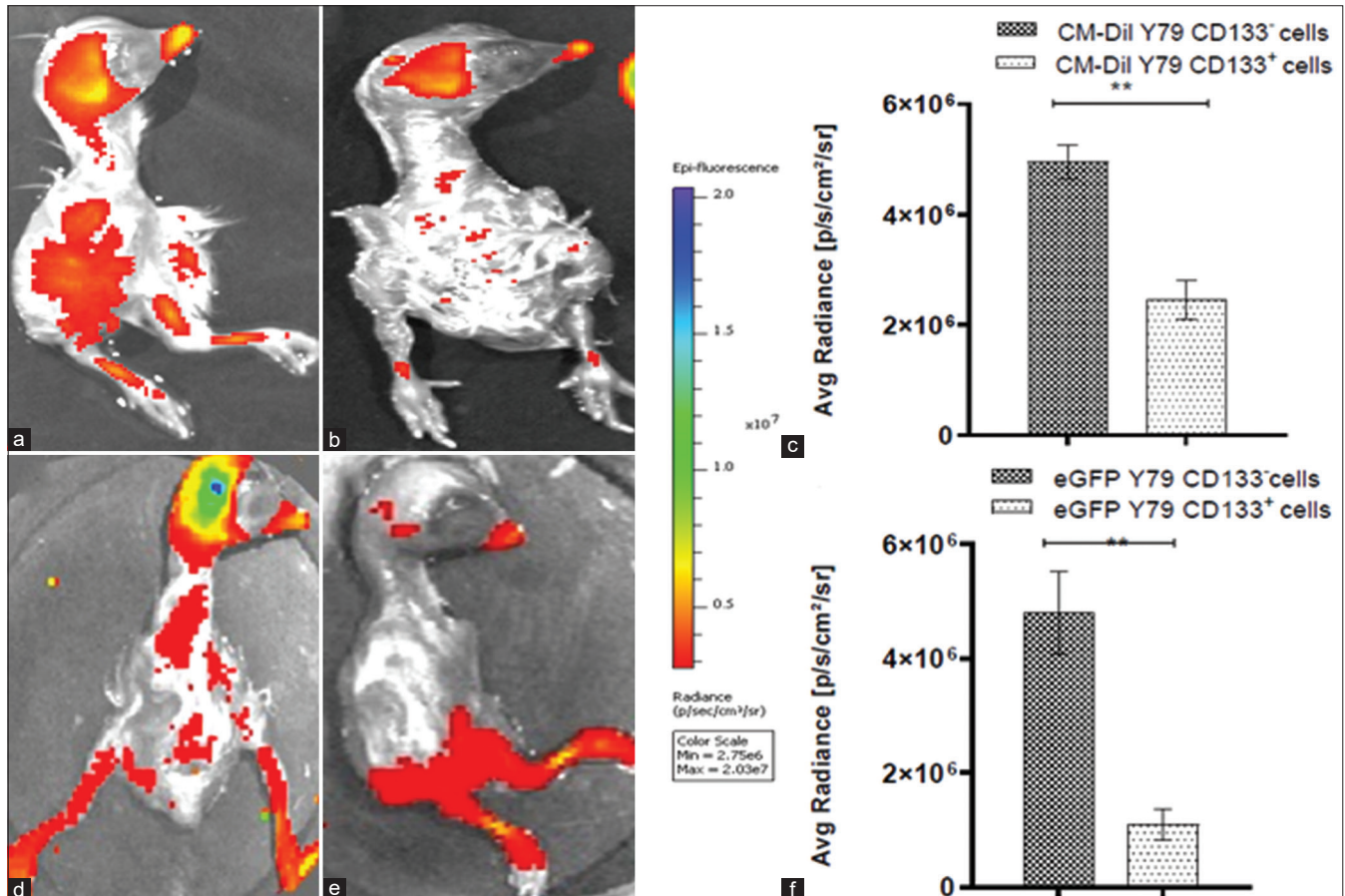


**Figure 5:** Evidence of Rb spontaneous metastasis in different parts of chick embryo analyzed using *in vivo* IVIS spectral imaging. Representative image of *in vivo* fluorescence observed in chick embryo transplanted with (a) CM-Dil Y79 CD133<sup>-</sup> cells, (b) CM-Dil Y79 CD133<sup>+</sup> cells, (d) eGFP Y79 CD133<sup>-</sup> cells, and (e) eGFP Y79 CD133<sup>+</sup> cells. Quantification of fluorescence intensity within the chick embryo revealed that CD133<sup>-</sup> cells had increased spontaneous metastasis when compared to CD133<sup>+</sup> cells (\*\**P* = 0.0077, 0.0017)

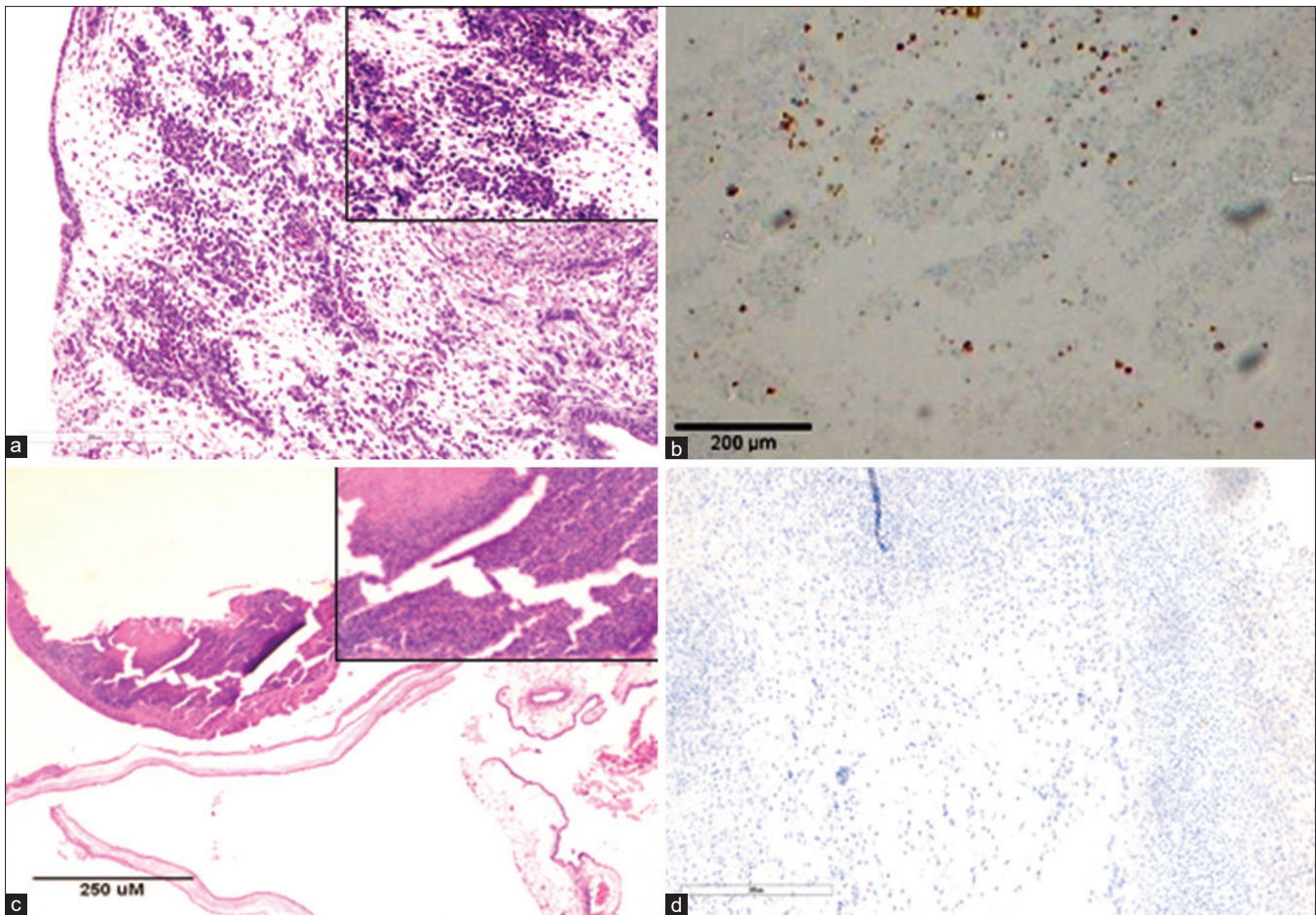


**Figure 6:** Histopathology of Rb Y79 CD133<sup>-</sup> and CD133<sup>+</sup> xenografts on the CAM layer (a) Histopathology of CAM transplanted with Y79 CD133<sup>-</sup> (CSCs) showed larger cells with increased N/C ratio. (b) The proliferating CD133<sup>-</sup> cells showed immunoreactivity with Ki-67. (c) Histopathology of CAM transplanted with Y79 CD133<sup>+</sup> (non-CSCs) showed multiple foci of tumor infiltrates, edema, and inflammation within the CAM stroma and (d) The Y79 CD133<sup>+</sup> cells were not reactive to the cellular proliferative marker, Ki-67

eye, and liver. Rb is clinically known to metastasize to the brain by invading through the optic nerve and to the bone and liver via hematogenous spread, and, therefore, involvement of the optic nerve, uvea, and sclera is considered as one of the important prognostic factors to predict metastasis.<sup>[1,24]</sup> Our findings also concur with the study done by Palmer and co-workers who investigated spontaneous metastasis of Human Epidermoid Carcinoma cell line (HEp3) to the chick liver and lung.<sup>[25]</sup> Though the imaging of CAM and embryo was possible after dissection, there was an observed signal in the beak area which did not reveal any presence of tumor cells upon histological analysis. This could be due to the autofluorescence from the bone and keratin present on the beak.

A further novel aspect of our study is the use of this model to study the tumorigenic and metastatic potential of CD133<sup>-</sup> CSCs within the Y79 cell line. This is an important validating point as the CD133<sup>+</sup> subset is projected as CSC in tumors of the brain,<sup>[26]</sup> while the negative cells seem to harbor CSC properties in Rb.<sup>[7]</sup> It would be logical to propose that while many CSC markers could be common to most tumors, some of them could vary in each tumor specifically due to the lineage of the tumor or specific aspects of differentiation of cells in that target tissue. For instance, CD133 is a marker of photoreceptor

differentiation<sup>[27]</sup>; hence, their precursor cells are expected to be negative for this marker, which we have documented both in primary and Y79 cell line.<sup>[7,20]</sup>

The CE-CAM model is an ideal short-term *in vivo* system to study different subsets of tumors and identify tumor-initiating cells. We also demonstrate the use of a cell tracker dye CM-Dil, with comparison to eGFP-labeled cells, to track Rb cells *in vivo*. CM-Dil dye has been successfully used earlier in the Rb zebrafish orthotopic xenograft model by Chen *et al.*,<sup>[28]</sup> who tracked the tumor cell invasion locally and along the optic nerve. However, considering that CM-Dil dye intensity could reduce with the proliferation of cells,<sup>[29]</sup> we also assessed the same using stable eGFP-labeled Y79 cells. GFP-labeled tumor cells were successfully used by several investigators to track *in vivo* metastases within the chick embryos in several tumors.<sup>[16,30,31]</sup> Our analyses showed that both the cell labeling strategies can be utilized for *in vivo* tracking. To the best of our knowledge, this is the first study that explores the use of *in vivo* fluorescence imaging of the whole embryo for identifying spontaneous metastasis in a CE-CAM Rb xenograft model.

The use of other alternate imaging technologies such as *in vivo* PET/CT has been demonstrated using radiotracers by Warnock *et al.*<sup>[32]</sup> in a glioblastoma xenograft model for studying

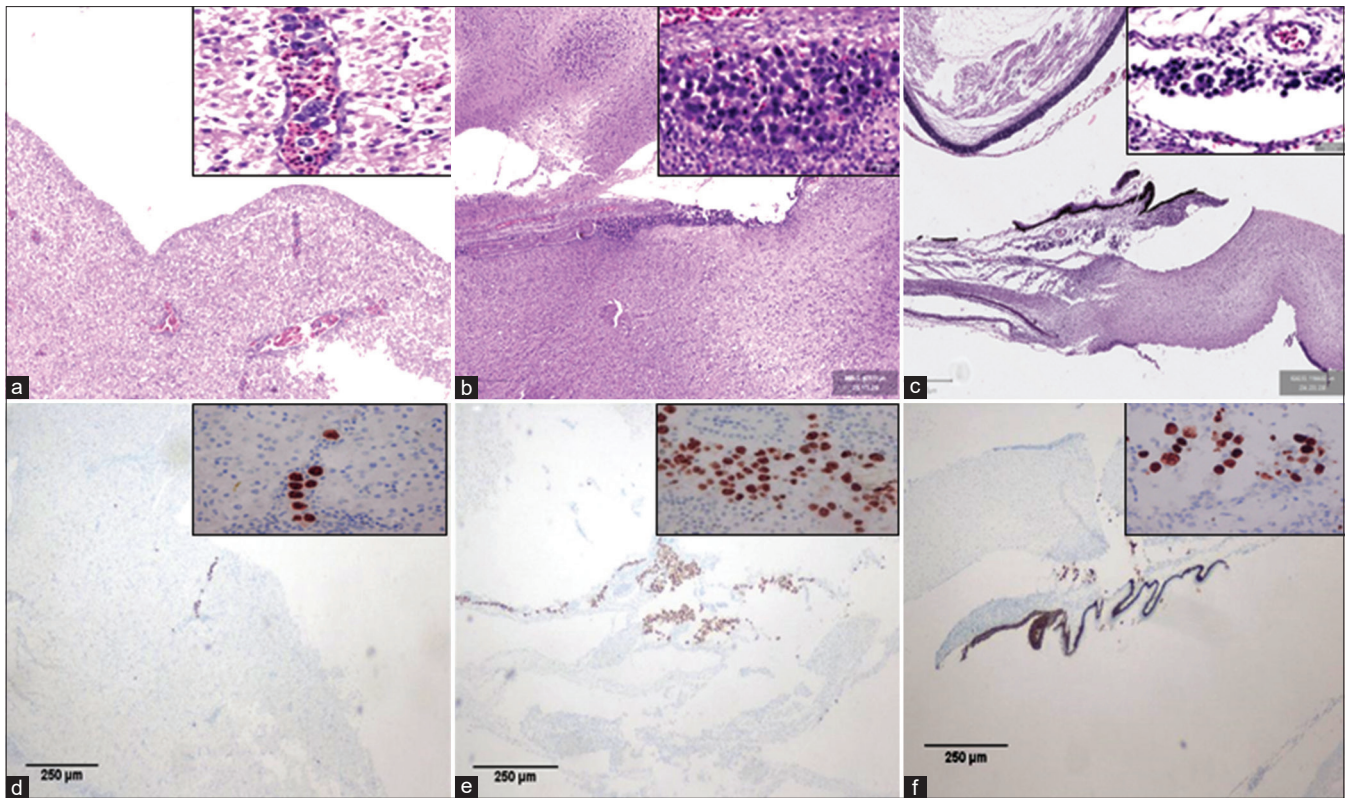


**Figure 7:** Histopathological evidence of metastasis into the embryonic organs. The embryos transplanted with Y79 CD133<sup>+</sup> cells show tumor cells within the (a) blood vessels of the liver (vascular emboli), (b) brain, and (c) eye. Immunohistochemical analysis of Ki-67 marker revealed positive cells within the (d) liver, (e) brain, and (f) eye

tumor metastasis. Their studies showed the PET tracer uptake over time by the tumor within the embryo and were able to measure the tumor volume with improved accuracy using CT imaging. The CE-CAM, owing to the ease of visualization through the window from the eggshell, makes it extremely suitable and convenient for tracking tumor cells *in vivo*.

The clinical relevance of this study is the use of an inexpensive, easy to establish *in vivo* model using cell lines and patient-derived xenografts for exploring existing and novel therapeutics. However, there are certain limitations of the CE model and further studies are required to understand cellular adaptations to the avian microenvironment. The incubation period of about a week may not be suitable for slow growing tumor cells, and it may be difficult to observe visible metastases in such cases. We believe that validating these results with early passage Rb primary cells and other Rb cell lines, WERI-Rb1, etc., in the future, would add more value to this *in vivo* model. The use of CM-Dil dye for tracking rapidly growing cells may be a challenge owing to its loss with each successive tumor generations, which could possibly under represent the tumor load of the tissue. Parallel confirmation with GFP-labeled Y79 cells helped overcome this limitation by demonstrating similar results in tumor formation and metastasis. Quantitative studies using human-specific gene expression assays could complement these assays in future.<sup>[25]</sup> Though the imaging of CAM and embryo was possible after dissection, the serial imaging of the entire live egg including the shell would be ideal for which different kinds of fluorescent dyes and standardization of the

software settings may be required, which we hope to address in our future studies.

## Conclusion

This study highlights that the Chick embryo-chorioallantoic membrane model is a simple short-term feasible alternative nonmammalian model for evaluating tumorigenicity and metastatic potential of Y79 cells as well as the properties of CSCs. Higher tumorigenicity and metastatic potential of Y79 CD133<sup>+</sup> subset of tumor cells support the CSCs properties in this subset of tumor cells. We speculate that this model system could serve as a valuable *in vivo* platform to understand Rb pathobiology as well as pave way for evaluating the CSC specific targeted therapies.

## Financial support and sponsorship

Nil.

## Conflicts of interest

There are no conflicts of interest.

## References

- Rodriguez-Galindo C, Orbach DB, VanderVeen D. Retinoblastoma. *Pediatr Clin North Am* 2015;62:201–23.
- Kaewkhaw R, Rojanaporn D. Retinoblastoma: Etiology, modeling, and treatment. *Cancers* 2020;12:2304.
- Dimaras H, Corson TW, Cobrinik D, White A, Zhao J, Munier FL, et al. Retinoblastoma. *Nat Rev Dis Primer* 2015;1:15021.
- Ancona-Lezama D, Dalvin LA, Shields CL. Modern treatment of

- retinoblastoma: A 2020 review. *Indian J Ophthalmol* 2020;68:2356–65.
5. Nimmakayala RK, Batra SK, Ponnusamy MP. Unraveling the journey of cancer stem cells from origin to metastasis. *Biochim Biophys Acta Rev Cancer* 2019;1871:50–63.
  6. Steinbichler TB, Savic D, Dudás J, Kvitsaridze I, Skvortsov S, Riechelmann H, *et al.* Cancer stem cells and their unique role in metastatic spread. *Semin Cancer Biol* 2020;60:148–56.
  7. Nair RM, Balla MMS, Khan I, Kalathur RKR, Kondaiah P, Vemuganti GK. *In vitro* characterization of CD133<sup>lo</sup> cancer stem cells in Retinoblastoma Y79 cell line. *BMC Cancer* 2017;17:779.
  8. Narayana RVL, Jana P, Tomar N, Prabhu V, Nair RM, Manukonda R, *et al.* Carboplatin- and etoposide-loaded lactoferrin protein nanoparticles for targeting cancer stem cells in retinoblastoma *in vitro*. *Invest Ophthalmol Vis Sci* 2021;62:13.
  9. Ruggeri BA, Camp F, Miknyoczki S. Animal models of disease: Pre-clinical animal models of cancer and their applications and utility in drug discovery. *Biochem Pharmacol* 2014;87:150–61.
  10. Nair RM, Kaliki S, Vemuganti GK. Animal models in retinoblastoma research. *Saudi J Ophthalmol* 2013;27:141–6.
  11. Nair RM, Vemuganti GK. Transgenic models in retinoblastoma research. *Ocul Oncol Pathol* 2015;1:207–13.
  12. Ribatti D. The chick embryo chorioallantoic membrane (CAM). A multifaceted experimental model. *Mech Dev* 2016;141:70–7.
  13. Murphy JB. Transplantability of tissues to the embryo of foreign species. *J Exp Med* 1913;17:482–93.
  14. Busch M, Philippeit C, Weise A, Dünker N. Re-characterization of established human retinoblastoma cell lines. *Histochem Cell Biol* 2015;143:325–38.
  15. Busch M, Papior D, Stephan H, Dünker N. Characterization of etoposide- and cisplatin-chemoresistant retinoblastoma cell lines. *Oncol Rep* 2018;39:160–72.
  16. Kalirai H, Shahidipour H, Coupland SE, Luyten G. Use of the chick embryo model in uveal melanoma. *Ocul Oncol Pathol* 2015;1:133–40.
  17. Kunz P, Schenker A, Sähr H, Lehner B, Fellenberg J. Optimization of the chicken chorioallantoic membrane assay as reliable *in vivo* model for the analysis of osteosarcoma. *PloS One* 2019;14:e0215312.
  18. Dyer MA. Lessons from retinoblastoma: Implications for cancer, development, evolution, and regenerative medicine. *Trends Mol Med* 2016;22:863–76.
  19. Seigel GM, Campbell LM, Narayan M, Gonzalez-Fernandez F. Cancer stem cell characteristics in retinoblastoma. *Mol Vis* 2005;11:729–37.
  20. Balla MMS, Vemuganti GK, Kannabiran C, Honavar SG, Murthy R. Phenotypic characterization of retinoblastoma for the presence of putative cancer stem-like cell markers by flow cytometry. *Invest Ophthalmol Vis Sci* 2009;50:1506–14.
  21. Große-Kreul J, Busch M, Winter C, Pikos S, Stephan H, Dünker N. Forced trefoil factor family peptide 3 (TFF3) expression reduces growth, viability, and tumorigenicity of human retinoblastoma cell lines. *PloS One* 2016;11:e0163025.
  22. Ribatti D. The chick embryo chorioallantoic membrane as a model for tumor biology. *Exp Cell Res* 2014;328:314–24.
  23. Ribatti D, Nico B, Pezzolo A, Vacca A, Meazza R, Cinti R, *et al.* Angiogenesis in a human neuroblastoma xenograft model: Mechanisms and inhibition by tumour-derived interferon-gamma. *Br J Cancer* 2006;94:1845–52.
  24. Dunkel IJ, Aledo A, Kernan NA, Kushner B, Bayer L, Gollamudi SV, *et al.* Successful treatment of metastatic retinoblastoma. *Cancer* 2000;89:2117–21.
  25. Palmer TD, Lewis J, Zijlstra A. Quantitative analysis of cancer metastasis using an avian embryo model. *J Vis Exp* 2011;51:2815.
  26. Schonberg DL, Lubelski D, Miller TE, Rich JN. Brain tumor stem cells: Molecular characteristics and their impact on therapy. *Mol Aspects Med* 2014;39:82–101.
  27. Lakowski J, Han Y-T, Pearson RA, Gonzalez-Cordero A, West EL, Gualdoni S, *et al.* Effective transplantation of photoreceptor precursor cells selected via cell surface antigen expression. *Stem Cells Dayt Ohio* 2011;29:1391–404.
  28. Chen X, Wang J, Cao Z, Hosaka K, Jensen L, Yang H, *et al.* Invasiveness and metastasis of retinoblastoma in an orthotopic zebrafish tumor model. *Sci Rep* 2015;5:10351.
  29. Progatzyk F, Dallman MJ, Lo Celso C. From seeing to believing: Labelling strategies for *in vivo* cell-tracking experiments. *Interface Focus* 2013;3:20130001.
  30. Carter R, Mullassery D, See V, Theocharatos S, Pizer B, Losty PD, *et al.* Exploitation of chick embryo environments to reprogram MYCN-amplified neuroblastoma cells to a benign phenotype, lacking detectable MYCN expression. *Oncogenesis* 2012;1:e24. doi: 10.1038/oncsis.2012.24.
  31. Herrmann A, Rice M, Lévy R, Pizer BL, Losty PD, Moss D, *et al.* Cellular memory of hypoxia elicits neuroblastoma metastasis and enables invasion by non-aggressive neighbouring cells. *Oncogenesis* 2015;4:e138–8.
  32. Warnock G, Turtoi A, Blomme A, Bretin F, Bahri MA, Lemaire C, *et al.* *In vivo* PET/CT in a human glioblastoma chicken chorioallantoic membrane model: A new tool for oncology and radiotracer development. *J Nucl Med* 2013;54:1782–8.